Bioactive Materials 6 (2021) 3496–3506

Contents lists available at ScienceDirect

Bioactive Materials

journal homepage: www.sciencedirect.com/journal/bioactive-materials

Bioactive glass promotes the barrier functional behaviors of keratinocytes and improves the Re-epithelialization in wound healing in diabetic rats

Fengling Tang [a,b,c], Junliang Li [b,c], Weihan Xie [a,b], Yunfei Mo [a,b,c], Lu Ouyang [a,b,c], Fujian Zhao [d], Xiaoling Fu [a,b,c,*], Xiaofeng Chen [a,b,c,**]

[a] Department of Biomedical Engineering, School of Materials Science and Engineering, South China University of Technology, Guangzhou 510641, PR China
[b] National Engineering Research Center for Tissue Restoration and Reconstruction, Guangzhou 510006, PR China
[c] Key Laboratory of Biomedical Engineering of Guangdong Province, and Innovation Center for Tissue Restoration and Reconstruction, South China University of Technology, Guangzhou 510006, PR China
[d] Stomatological Hospital, Southern Medical University, Guangzhou 510280, PR China

ARTICLE INFO

Keywords:
Bioactive glass
Keratinocyte
Barrier function
Diabetic wound healing

ABSTRACT

Upon skin injury, re-epithelialization must be triggered promptly to restore the integrity and barrier function of the epidermis. However, this process is often delayed or interrupted in chronic wounds like diabetic foot ulcers. Considering that BG particles can activate multiple genes in various cells, herein, we hypothesized that bioactive glass (BG) might be able to modulate the barrier functional behaviors of keratinocytes. By measuring the transepithelial electrical resistance (TEER) and the paracellular tracer flux, we found the 58S-BG extracts substantially enhanced the barrier function of keratinocyte monolayers. The BG extracts might exert such effects by promoting the keratinocyte differentiation and the formation of tight junctions, as evidenced by the increased expression of critical differentiation markers (K10 and involucrin) and TJ protein claudin-1, as well as the altered subcellular location of four major TJ proteins (claudin-1, occludin, JAM-A, and ZO-1). Besides, the cell scratch assay showed that BG extracts induced the collective migration of keratinocytes, though they did not accelerate the migration rate compared to the control. The in vivo study using a diabetic rat wound model demonstrated that the BG extracts accelerated the process of re-epithelialization, stimulated keratinocyte differentiation, and promoted the formation of tight junctions in the newly regenerated epidermis. Our findings revealed the crucial effects of BGs on keratinocytes and highlighted its potential application for chronic wound healing by restoring the barrier function of the wounded skin effectively.

1. Introduction

One of the most important functions of the skin is to provide a physical protective barrier for our bodies against the external environment [1]. It is now generally accepted that the barrier function of the skin resides in the epidermis and mainly due to the stratum corneum and tight junctions (TJs) between keratinocytes [2]. The stratum corneum is the outermost layer of the epidermis and is made up of terminally differentiated enucleated keratinocytes (also known as "corneocytes"). The enucleated keratinocytes in the stratum corneum organize in a brick and mortar formation within a lipid-rich extracellular matrix to help defend us against dehydration, toxins, and bacteria. On the other hand, TJs, consisting of transmembrane proteins (claudins, occludin, junctional adhesion molecules (JAMs)) and cytosolic plaque proteins (zonula occludens (ZO)), extend from adjacent keratinocytes to form paired strands that seal the paracellular pathway thus restricting the diffusion of molecules through the intercellular space [3,4].

Upon skin injury, as the barrier is disrupted, a process termed re-epithelialization must be triggered promptly to restore the epidermis structure and its barrier function. Thus, re-epithelialization is incredibly important and has been used as a defining parameter of the wound healing success. However, this critical event is impaired in all types of chronic wounds, providing a portal for wound infection. As a result, a substantial proportion of chronic wounds suffer from severe infection

Peer review under responsibility of KeAi Communications Co., Ltd.
* Corresponding author. National Engineering Research Center for Tissue Restoration and Reconstruction, Guangzhou 510006, PR China.
** Corresponding author. National Engineering Research Center for Tissue Restoration and Reconstruction, Guangzhou 510006, PR China.
E-mail addresses: msxlfu@scut.edu.cn (X. Fu), chenxf@scut.edu.cn (X. Chen).

https://doi.org/10.1016/j.bioactmat.2021.02.041
Received 4 January 2021; Received in revised form 26 February 2021; Accepted 26 February 2021

and wound reoccurrence. While many factors may contribute to the impaired re-epithelialization in chronic wounds, the dysfunction of keratinocytes is undoubtedly a crucial one. It has been shown that keratinocytes at the margins of chronic diabetic wounds, though highly proliferative, are difficult to differentiate and form stable layered structures [5]. Besides, the hyperglycemic condition stimulates the production of reactive oxygen species (ROS), which reduces the epithelial barrier integrity via inhibiting the formation of TJs [6,7]. Two major TJ proteins, claudin-1 and occludin, were also found suppressed at the wound margins and in the regenerated epidermis [8]. Thus, therapies that modulate the phenotype of keratinocytes, helping achieve re-epithelialization and restore the barrier function, would benefit to the healing process of the chronic wounds.

Bioactive glasses (BGs), a type of silicate-based inorganic material, are typically composed of Na_2O, SiO_2, CaO, and P_2O_5. Recently, BGs have been used to treat wounds and shown massive potential in the field of cutaneous wound healing. Numerous studies have explored the effects of BGs on wound healing-related cells. It has been reported that BGs not only promote the migration of fibroblasts but also up-regulate the secretion of growth factors, as well as the production of the extracellular matrix [9]. Besides, BGs can polarize macrophages towards the M2 phenotype, thus modulating the inflammatory responses of wound healing [10,11]. BGs can also promote the expression of angiogenic genes in HUVECs and stimulate the gap junction of HUVECs to enhance neovascularization [12,13]. However, the effects of BGs on keratinocytes remain unclear. **Since** the soluble ions (e.g., Si, Ca, and P) released by BGs particles can activate multiple signal transduction pathways in various cells [14], we hypothesize that BG may be able to modulate the barrier functional behaviors of keratinocytes.

In this study, the ionic extracts from 58S-BG were used as a model to investigate the effects of BGs on keratinocytes. The barrier function of keratinocyte monolayers after treatment with the BG extracts was evaluated through measuring the transepithelial electrical resistance (TEER) and the selective paracellular permeability. To reveal the mechanism through which the BG extracts modulate the barrier function, the differentiation of keratinocytes and the TJs formed between keratinocytes were systematically examined. Moreover, the BG extracts were applied onto the full-thickness cutaneous wounds in diabetic rats to investigate their effects on the barrier restoration and overall outcomes of wound healing.

2. Experimental section

2.1. Cell culture

Human Neonatal Foreskin Epidermal Keratinocytes were purchased from American Type Culture Collection (ATCC, USA). Keratinocytes were cultured in the keratinocytes culture medium, consisting of Dermal Cell Basal Medium (ATCC, USA) supplemented with Keratinocyte Growth Kit and Penicillin-Streptomycin-Amphotericin B Solution, in a humidified 37 °C, 5% CO_2 incubator (Thermo Scientific, USA). The medium was refreshed every 3 days until the cells were confluent. When the confluence reached approximately 70%–80%, cells were passaged using Primary Cells Trypsin-EDTA (ATCC, USA). Only early passages (passages 3–7) of the Keratinocytes were used in this study.

2.2. Preparation and characterization of BG particles and BG extracts

BG particles with a molar composition of 60% SiO_2, 36% CaO, and 4% P_2O_5 were synthesized by Sol-gel method as described previously [15]. Ethyl tetraethyl orthosilicate (TEOS), Ttriethylphosphate (TEP), calcium nitrate tetrahydrate ($Ca(NO_3)_2{\cdot}4H_2O$), deionized water and hydrochloric acid were purchased from Guangzhou Chemical Reagent Factory. According to the molar composition, 10.24 g TEOS, 1.16 g TEP, 7.02 g $Ca(NO_3)_2{\cdot}4H_2O$ were added in order with stirring to a solution containing 7.82 g water and 1.30 g hydrochloric acid (2 M). The above mixture was continuously stirred until it became homogeneous sol, and the sol was solidified into transparent gel at room temperature in 72 h. The gel was then aged at 60 °C for three days, followed by drying at 120 °C for 3 h. Templates and organic components were removed by sintering at 650 °C for 3 h. Finally, the BG particles were obtained after ball-milling, drying, and sieving (400 mesh).

The morphology of BG particles was examined with a field emission scanning electron microscope (FE-SEM, Merlin Carl Zeiss Jena, Germany). The particle size distribution was analyzed using a Zetasizer Nano ZS (Malvern Instruments, UK). The chemical structure and phase composition of BG particles were characterized by Fourier transform infrared spectroscopy (FTIR; Vector 33, Bruker, Germany) and X-ray diffraction (XRD, X'Pert^3 Powder, PANalytical, Netherlands). The specific surface area was measured using the multipoint Brunauer–Emmett–Teller (BET) N2 absorption technique (BET, NOVA4200e, Quantachrome, USA) at 77.3 K. The pore diameter distribution of the BG particles was evaluated from the desorption branch of the isotherms by the density functional theory (DFT) method.

To prepare the ionic extracts from BG particles, 1 g sterilized BG powder was placed in a 10 cm diameter culture dish and soaked in 5 ml Dermal Cell Basal Medium (ATCC, USA). Afterward, the mixture was incubated in a cell culture incubator containing 5% CO_2 at 37 °C. After 24 h, the BG extracts were obtained by centrifugation and filtration (Millipore, 0.22 mm). For further cell culture, BG extracts were diluted at ratios of 1/20, 1/80, and 1/320 with the keratinocytes culture medium (hereafter referred to as 1/20, 1/80 and 1/320, respectively). The concentrations of Si, Ca, and P ions were analyzed by inductively coupled plasma atomic emission spectrometer (ICP-AES, PS1000-AT, Leeman, USA).

2.3. Cell proliferation

Cell proliferation was determined using a Cell Counting Kit-8 (CCK-8, Dojindo Laboratories, Japan) following the protocol suggested by the manufacturer. Keratinocytes were seeded at a density of 3000 cells/well in a 96-well plate. After cells have adhered, the culture medium was replaced by the diluted BG extracts, and the keratinocyte culture medium without BG extracts was used as the control. The culture medium of each group was refreshed every 3 days. The cells were harvested on days 1, 3, and 7 for CCK-8 assay. After washing three times with DPBS, the cells were incubated in keratinocyte culture medium containing 10% CCK-8 reagent at 37 °C for 2.5 h. The absorbance of each sample was measured at 450 nm by a Thermo Scientific Microplate Reader (Thermo 3001, USA).

2.4. Cell migration

Cell migration was determined by the cell scratch assay. Keratinocytes were seeded into 24-well plates and allowed to grow until they almost formed confluent monolayers. In order to exclude any effects from cell proliferation, cells were pretreated with the anti-proliferative agent mitomycin C (10 μg/L) for 2 h [16]. A straight vertical scratch was made down through the keratinocyte monolayers by using a 1 ml plastic pipette tip. The cells were then cultured with the diluted BG extracts and the keratinocyte culture medium, respectively. The gap was imaged using a microscope equipped with a digital camera at 0 and 24 h. The area of the gap was measured using Image J. The cellular migration rate was calculated according to the following equation: migration rate (%) = $St/S_0 \times 100\%$ (S_0 initial gap area, St: cell covered area amid the gap at time t).

2.5. Measurement of transepithelial electrical resistance

Transepithelial electrical resistance (TEER) is a widely accepted quantitative technique to measure the barrier integrity [17]. A higher TEER indicates a better barrier function. The in vitro TEER measurement

was performed following the protocol described previously. Briefly, 8×10^4 keratinocytes were seeded on the polyester filter membrane of a transwell device (24-well format, 0.4 mm pore size, Corning, USA) and cultured in the diluted BG extracts and the control medium, respectively. The TEER value was measured using a Millicell ERS-2 epithelial volt-ohmmeter (Millipore, USA) on days 1, 3, 7. The net value of each group was calculated by subtracting the background value, which was measured on the cell-free filter membrane, from the value of each group [18].

2.6. Paracellular permeability assay

In order to evaluate the selective paracellular permeability of the keratinocyte monolayers after culturing with the diluted BG extracts, a permeability assay was conducted with fluorescein isothiocyanate-labeled dextran (FITC-dextran, 4 kDa, Sigma-Aldrich, USA) [19]. 8×10^4 keratinocytes were cultured on the polyester filter membrane of a transwell device (24-well format, 0.4 mm pore size, Corning, USA) and cultured in the diluted BG extracts and the control medium, respectively. The paracellular flux was measured at 24, 48, and 72 h. At each time point, the monolayers were gently washed with DPBS, and the medium in the apical and basal chambers was gently replaced with 200 μL of DPBS containing 1 mg/mL of FITC–dextran and 600 μL of DPBS, respectively. Then, the transwell devices were incubated at 37 °C for 2 h. Afterward, 100 μL sample was collected from the basal chamber for fluorescence determination using a Thermo Scientific Microplate Reader (Thermo 3001, USA) at an excitation wavelength of 480 nm and an emission wavelength of 520 nm. To facilitate comparisons between different groups, the paracellular flux of each group was normalized to that of the control [19].

2.7. Real-time quantitative PCR (RT-qPCR)

The relative mRNA levels related to keratinocyte differentiation and TJs was determined via quantitative real-time polymerase chain reaction (qRT-PCR) as described previously. Total RNA of the keratinocytes was extracted using HiPure Total RNA Micro Kit (Magen, China). The extracted RNA was then reverse transcribed into cDNA using the Reverse Transcription Reagent Kit (Takara, Japan) according to the manufacturer's protocol. The quantitative real-time PCR was performed with the QuantStudio 6 Flex system (Life Technologies, USA) using Maxima SYBR Green/ROX qPCR Master Mix (Thermo Scientific, USA). Gene expression was quantified using the ΔΔCt method, and the fold change was calculated using formula $2^{-\Delta\Delta Ct}$. Values of the genes were normalized to the house-keeping gene GAPDH. The primer sequences used in this study are presented in Table S1 (Supporting Information).

2.8. Immunofluorescence assay

Keratinocytes cultured with diluted BG extracts were harvested until they reached confluence. After fixation with 4% paraformaldehyde for 30 min, the cells were permeabilized with 0.1% Triton X-100 and blocked with 5% (wt/vol) bovine serum albumin at room temperature. Afterward, the cells were incubated with the primary antibody at 4 °C overnight. Primary antibodies used in the study were as follows: anti-keratin-10 (Abcam, USA, 1:100), anti-Claudin-1 (Abcam, USA, 1:100), anti-Occludin (Invitrogen, USA, 1:100),anti-ZO-1 (Invitrogen, USA, 1:100) or anti-JAM-A (R&D Systems, USA, 1:100). Then, the cells were washed with DPBS and incubated with Alexa Fluor®488-conjugated secondary antibody (Abcam, USA, 1:1000) for 1 h at room temperature in dark. Cell nuclei were stained with DAPI (Beyitime, China, 1:1000) for 10 min. The stained cells were observed by a confocal laser scanning microscopy (CLSM, Leica SP8, Germany).

2.9. Western blotting analysis

Keratinocytes were collected and lysed in RIPA lysis buffer (Beyotime, China). Concentrations of the whole protein were determined using a BCA protein assay kit (Thermo Scientific, USA). Approximately 15–20 μg of proteins from each sample were separated by SDS-PAGE on 12% stain-free gels (TGX Stain-Free™ FastCast™ Acrylamide kit, Bio-Rad, USA) and transferred to PVDF membranes (Millipore, USA). The membranes were blocked with 5% BSA (Sigma Aldrich) and incubated with primary antibodies at 4 °C overnight. The primary antibodies used in western blotting included anti-keratin 14 (Santa Cruz Biotechnology, USA, 1:1000),anti-keratin 10 (Abcam, USA, 1:10000), anti-involucrin (Abcam, USA, 1:1000), anti-Claudin-1 (Abcam, USA, 1:1000), anti-Occludin (71–1500, Invitrogen, USA, 1:1000), anti-ZO-1 (Invitrogen, USA, 1:1000), anti-JAM-A (R&D Systems, USA, 1:2500), and anti-GAPDH(Signalway Antibody, USA, 1:2000). Subsequently, the membranes were washed and incubated with HRP-conjugated secondary antibody (Signalway Antibody, USA) for 1 h at room temperature. The immunoreactive protein bands were detected using the chemiluminescent reagent (Clarity Western ECL, Bio-Rad, USA). The signals were visualized by the ChemiDoc ™Touch Imaging System (Bio-Rad, USA). The intensities of the visualized bands were then quantified by densitometry and normalized to GAPDH.

2.10. In vivo study

2.10.1. Induction of type I diabetic rat model

All animal procedures were approved by the Animal Care and Use Committee of Guangdong Pharmaceutical University. 36 healthy Sprague-Dawley (SD) rats weighing 250–300 g were purchased from the experimental animal center of Guangdong Pharmaceutical University, Guangzhou. Diabetes was induced by intravenously injecting 1% streptozotocin (STZ, 65 mg/kg) dissolved in 0.1 M sodium citrate buffer. After 7 days, STZ-treated rats showing blood glucose levels higher than 16.7 mM, together with weight loss, polyuria and polydipsia, were considered as successful type I diabetic rat models. All rats were kept in a specific pathogen-free (SPF) environment and were fed a standard diet.

2.10.2. Treatment of full-thickness skin wounds in diabetic rats by BG extracts

Diabetic rats were anesthetized with an intraperitoneal injection of 1% pentobarbital sodium (30 mg/kg) and operated under sterile conditions. After shaving and sterilization, two circular, full-thickness skin wounds (Φ 18 mm) were created on the back of each rat (Fig. S1) as described previously [20]. The two diabetic skin wounds of each rat were randomly received different treatments. Accordingly, the wounds were assigned into three groups, including 1/20, control and blank. In the 1/20 group, 100 μL of the 1/20 BG extract was injected subcutaneously along the margin of the wound at six injection sites, whereas an equivalent volume of keratinocyte culture medium was administered in the control group in the same fashion. Wounds without any treatment were set as the blank group. All wounds were covered with Tegaderm™ transparent film (3 M Health Care, Germany). All rats were maintained in individual cages and fed a standard diet after surgery. The healing status of the wounds in each group was observed by photographing the wound areas on day 3, 7,14, and 21 after surgery. Images of the wounds were captured by a digital camera and measured by Image J. The wound healing rate was calculated according to the following equation: healing rate $= (A_0\text{-}A_t)/A_0 \times 100\%$, where A_0 represents the initial wound area and A_t represents the wound area at time t.

2.10.3. Histology analysis

Rats were sacrificed on days 7, 14, and 21 after various treatments. For the histological study, the wound samples were fixed in 4% paraformaldehyde for 24 h, embedded in paraffin, and then cut into 5 μm sections using a rotary microtome (RM2016, Leica, Germany). The

sections were deparaffinized and rehydrated, and further stained with hematoxylin-eosin (H&E). Histological images were taken using a Pannoramic 250 Flash series digital scanner (P250 FLASH, 3DHISTECH, Hungary).

2.10.4. Immunohistochemical and immunofluorescence staining

For immunohistochemical analysis, the rehydrated tissue sections were immersed with 3% H_2O_2 and 80% carbinol for 15 min and heated in 10 mM citrate buffer twice, followed by treating with 5% bovine serum albumin (BSA) (Beyotime) for 1 h. The samples were then incubated with primary antibodies against Keratin 14 (Santa Cruz, USA, 1: 100), keratin 10(Abcam, USA, 1: 100), involucrin (Santa Cruz, USA, 1: 100) and Ki-67 (Abcam, USA, 1: 100) at 4 °C overnight. After several washes with PBS, they were incubated with EliVision™ super/HRP secondary antibody (Fuzhou Maixin Biotech, China). The antibody binding sites were visualized by incubating with diaminobenzidine (DAB) (ZSGB-BIO, Beijing, China) in PBS, and the sections were counterstained with hematoxylin counterstaining. The staining was examined using a Pannoramic 250 Flash series digital scanner (P250 FLASH, 3DHISTECH, Hungary). For immunofluorescent analysis, the rehydrated tissue sections were incubated with 5% bovine serum albumin (BSA) (Beyotime) for 1 h to block nonspecific binding. Then, the samples were stained with primary antibody anti-claudin-1 (Abcam, USA, 1: 100), anti-occludin (Invitrogen, USA, 1:100), anti-ZO-1 (Invitrogen, USA, 1:100) or anti-JAM-A (R&D Systems, USA, 1:100) at 4 °C overnight. Excess antibodies were removed by washing with PBS, followed by incubating with HRP-conjugated Alexa Fluor®647-conjugated secondary antibody (Abcam, USA, 1:1500) at room temperature for 1 h. Cell nuclei were stained by DAPI (Beyotime). All fluorescent images were taken using a Pannoramic 250 Flash series digital scanner (P250 FLASH, 3DHISTECH, Hungary). The staining images were then quantitatively analyzed using image J (v1.53).

2.10.5. Statistical analysis

All experiments were performed in triplicate and repeated independently at least 3 times. Data are expressed as means ± standard deviation (SD). The statistical analysis was done with Graphpad Prism 6 software. One-way analysis of variance (ANOVA) with Tukey's multiple comparison test was used to analyze differences between the experimental groups. A P value below 0.05 was considered to indicate a statistically significant difference.

3. Results

3.1. Characterization of BG particles and BG extracts

The BG particles were successfully synthesized using the sol-gel method. The SEM images showed that the BG particles, which had irregular morphologies, were aggregates of many nanoparticles (Fig. 1a). The particle sizes were mainly distributed within the 5 μm–15 μm range (Fig. 1b). The XRD analysis and the FTIR results confirmed that the obtained BG particles presented the representative amorphous feature and Si–O–Si composition (Fig. 1c and d). The specific surface area (SSA) and pore structure of the BG particles were obtained by the N_2 absorption-desorption isotherm (Fig. 1e and f). The SSA, pore volume, and mean pore diameter of the BG particles were 121.287 $m^2\ g^{-1}$, 0.248 $cm^3\ g^{-1}$, and 6.079 nm, respectively (Fig. 1g).

The concentrations of Ca, Si, and P ions in the BG extracts were detected, and the results are presented in Table 1. There was little difference between the concentration of P ions in the BG extracts and the control. However, the levels of Ca and Si ions in the BG extracts were

Table 1
Ca, Si and P ions concentration of BG extracts.

	Ca (mg/L)	P (mg/L)	Si (mg/L)
Control	2.468 ± 0.035	69.440 ± 0.388	0.043 ± 0.003
1/20	28.858 ± 0.344	66.025 ± 0.356	2.691 ± 0.011
1/80	9.429 ± 0.080	68.608 ± 0.205	0.703 ± 0.006
1/320	4.352 ± 0.035	68.911 ± 0.384	0.188 ± 0.005

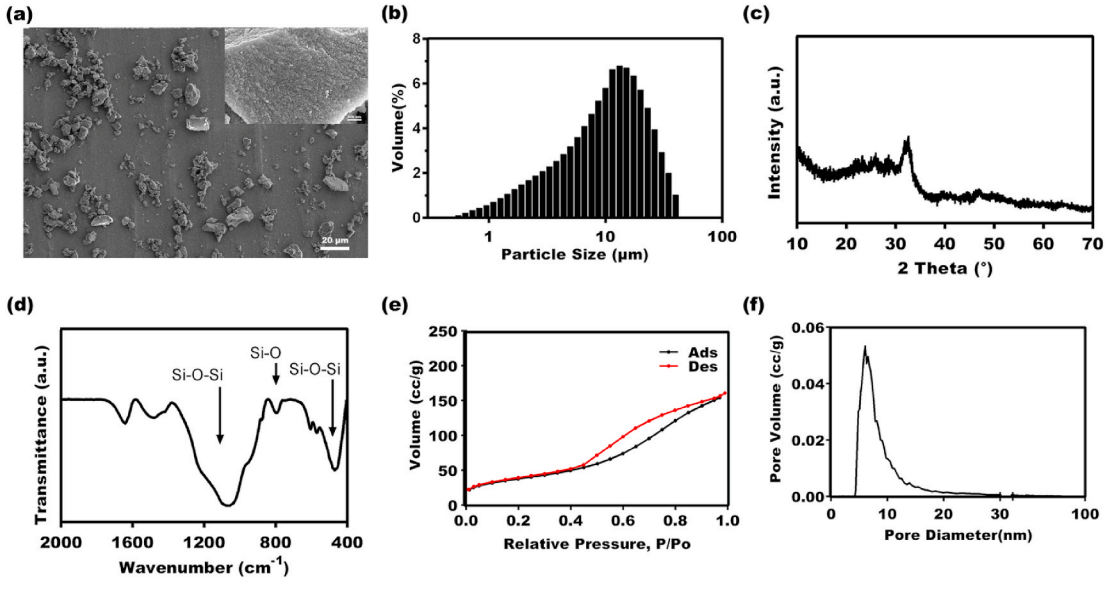

Fig. 1. Characterization of BG. (a) SEM image of BG. (b) Particle size distribution of BG. (c) XRD pattern of BG. (d) FTIR spectra of BG. (e) The nitrogen adsorption-desorption isotherms of BG. (f) Pore size distribution of BG. (g) Surface pore structures of BG.

significantly higher than those in control.

3.2. Effects of BG extracts on the proliferation of keratinocytes

For cell proliferation evaluation, keratinocytes were incubated in BG extracts for 1,3,7 days. In the first 3 days, cells cultured in BG extracts exhibited a similar growth pattern as in control (Fig. 2a), with no significant difference between the groups. This trend continued for the next four days for the 1/80 and 1/320 groups. However, the OD value of the 1/20 group was much lower than the control, indicating that BG extracts diluted at the ratio of 1/20 suppressed the proliferation of keratinocytes.

3.3. Effects of BG extracts on the migration of keratinocytes

As shown in Fig. 2b, a large number of migrated cells were observed in the scratch area of each group after 24 h. Quantitative statistical analysis showed that the migration rates of the 1/20 group (48.30 ± 2.795%), the 1/80 group (58.01 ± 1.494%) and the 1/320 group (53.6 ± 5.799%) were close to that of the control group (55.75 ± 5.277%), with no statistical difference between the groups (Fig. 2c). However, it was noted that cells in the scratch area of the control group were scattered with no visible cell-cell contacts between each other, suggesting a single-cell migration. On the contrary, cells cultured in the BG extracts migrated collectively like sheets. The majority of cells retained their cell-cell contacts when they moved forward.

3.4. BG extracts enhanced the barrier function of keratinocytes monolayer

Both TEER and paracellular permeability of FITC–dextran was determined to evaluate the effects of the BG extracts on the barrier function of the keratinocyte monolayers (Fig. 3). The TEER values of the keratinocyte monolayers cultured in the BG extracts were significantly higher compared to that of the control group during the whole culturing period (Fig. 3a). On day 1, the TEER values of the 1/20, 1/80 and 1/320 group were 22.51 ± 2.73 Ω cm^2, 19.43 ± 3.42 Ω cm^2, and 9.827 ± 0.89 Ω cm^2, respectively, whereas that of the control group was only 8.653 ± 0.80 Ω cm^2. After seven days, the TEER values of 1/20, 1/80 and 1/320 group increased to 1541 ± 50.94 Ω cm^2, 670.0 ± 14.12 Ω cm^2, and 120.3 ± 8.19 Ω cm^2, respectively. However, the TEER value in control was merely 15.18 ± 0.83 Ω cm^2. Apparently, the BG extracts enhanced the TEER of the keratinocyte monolayer. Such effect seemed directly related to the concentration of the BG extracts because the 1/20 group induced the most significant improvement in the TEER. Consistently, the paracellular flux of FITC-dextran tracer (4 kDa) across the keratinocyte monolayers in the BG extracts was remarkedly reduced compared to in control at every time point (Fig. 3b). These results demonstrated that BG extracts enhanced the barrier function of the keratinocyte monolayers.

3.5. BG extracts promoted the differentiation of keratinocytes

The differentiation of keratinocytes resulted in the formation of stratum corneum, thus plays a vital role in maintaining the skin barrier function. The effects of the BG extracts on keratinocyte differentiation were evaluated by examining key differentiation markers, including Keratin (K) 14, 10, and involucrin. Keratinocytes in the basal layer are proliferative and express K14. As keratinocytes move toward the surface traversing layers known as the spinous layer and granular layer, they undergo the process of differentiation and switch to express K10 [21]. Involucrin is a marker of early terminal differentiation in keratinocytes [22]. As shown in Fig. 4a, the gene expressions of K10 and involucrin in keratinocytes were significantly up-regulated by the BG extracts, with

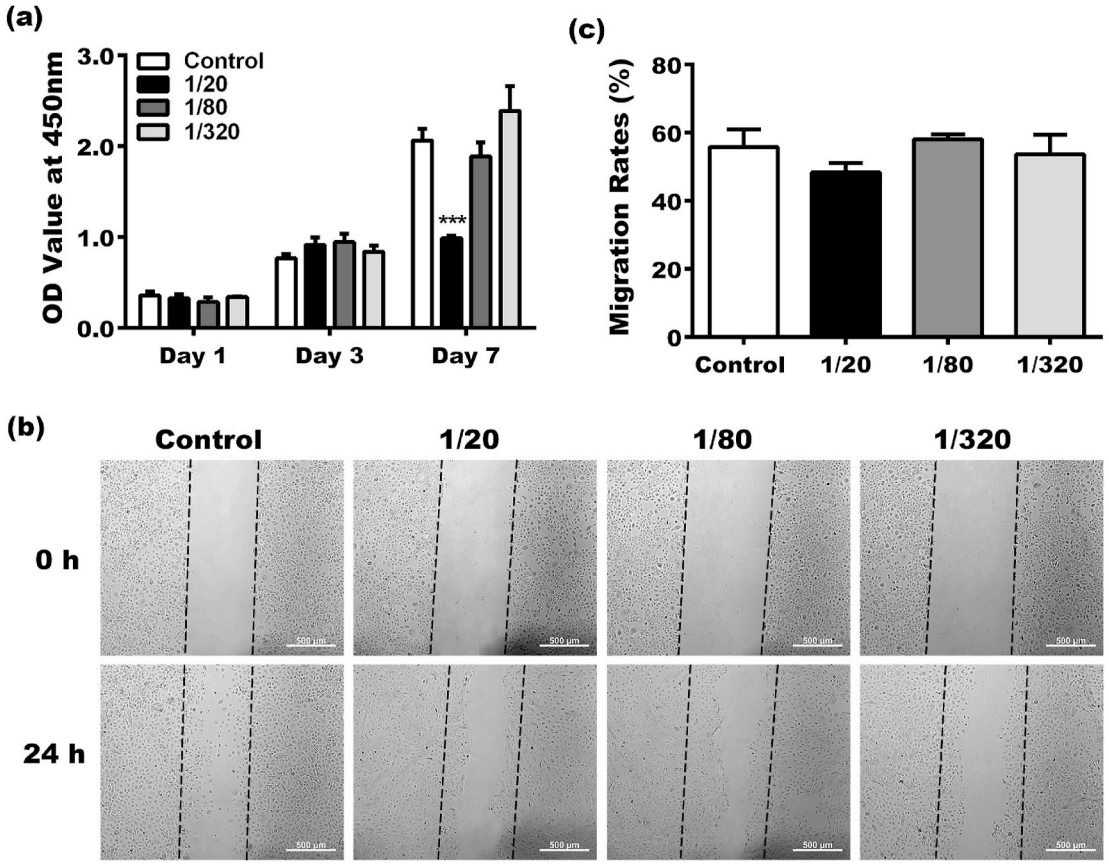

Fig. 2. (a) The effect of BG on the proliferation of keratinocytes. (b) Images of cell scratch assay for migration of keratinocytes cultured for 0 and 24 h. (c) Quantitative results of the migrated keratinocytes in the cell scratch assay. (*Statistically significant, ***$p < 0.001$ vs the control group).

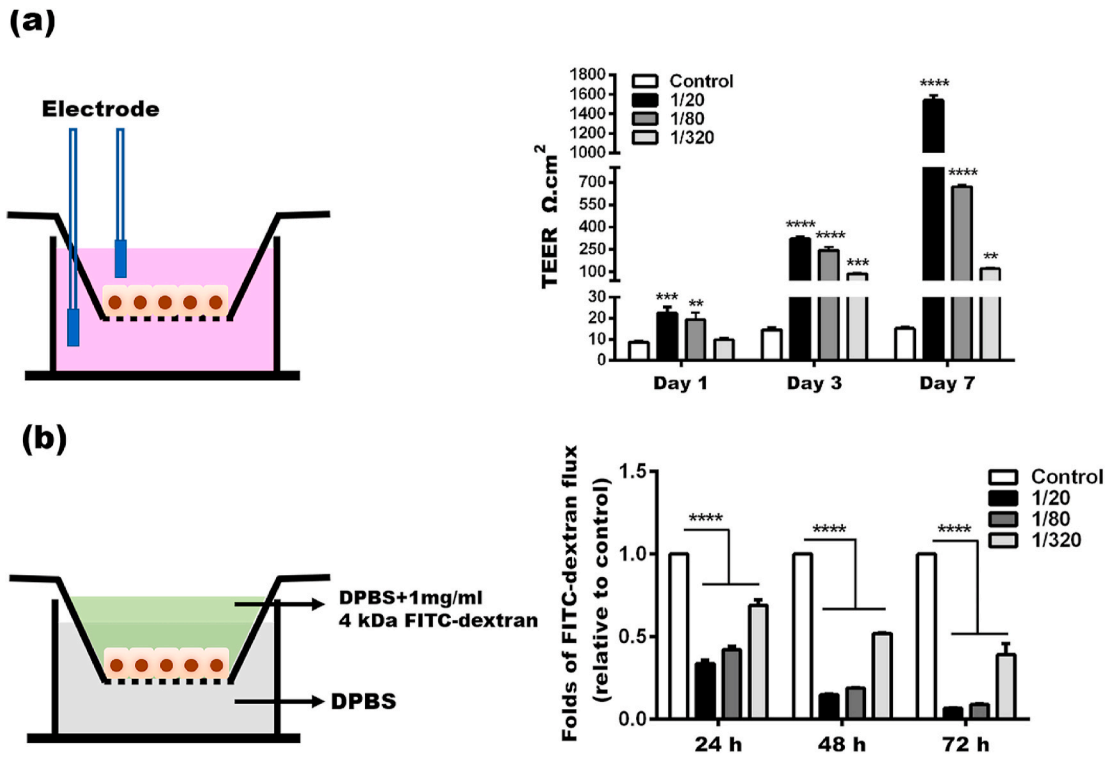

Fig. 3. The barrier function of keratinocyte monolayers in the BG extracts. (a) The TEER of keratinocyte monolayers. (b) The paracellular permeability of keratinocyte monolayers. (*Statistically significant, **p < 0.01, ***p < 0.001, ****p < 0.0001 vs the control).

expression in 1/20 group being the highest. In contrast, the level of K14 was comparable in each group. Our Western blot analysis further confirmed that keratinocytes cultured in the BG extracts expressed remarkedly higher levels of K10 and involucrin than those in control, especially K10 (Fig. 4b). As expected, more K10 positive cells were observed as the concentration of the BG extracts raised (Fig. 4c), while very few K10 positive cells were found in control. These results showed that BG extracts promote the differentiation of keratinocyte.

3.6. BG extracts enhance TJ integrity

Tight junction formed between keratinocytes is another critical component that maintains the barrier function of the skin. Thus, we next determined the expression and localization of tight junction-associated proteins in keratinocytes in the BG extracts. The gene expression of Claudin-1 and occludin was significantly up-regulated in the 1/20 and 1/80 groups compared to that in the 1/320 group and control. However, no significant difference in ZO-1 and JAM-A was observed between the groups of BG extracts and the control (Fig. 5a). Interestingly, according to Western blot analysis, only claudin-1 was elevated in the 1/20 and 1/80 groups compared to the control, whereas JAM-A was down-regulated in keratinocytes in BG extracts (Fig. 5b). Tight junction is formed by the assembly of multiple TJ proteins between neighboring cells. Thus, the location of the TJ proteins is an evenly important parameter when evaluating the TJ integrity. As shown in Fig. 5c, the majority of TJ proteins, including ZO-1, occludin, JAM-A, and claudin-1, were located along the cell membrane of keratinocytes in the BG extracts, suggesting the formation of TJs. On the contrary, TJ proteins in keratinocytes in control seemed to fail to assemble into TJs between adjacent cells. These results illustrated that BG extracts enhanced TJ integrity in keratinocyte monolayers by modulating the expression and localization of TJ proteins.

3.7. Effects of BG extracts on diabetic wound healing

3.7.1. Gross observation and histological analysis of diabetic wounds

Fig. 6a showed representative images of the full-thickness wounds at day 0, 3, 7,14, and 21 after receiving different treatments. The photographic evaluation clearly illustrated a faster, better healing process in wounds treated with 1/20 BG extracts. On day 3, the wound sizes in all groups decreased to a similar size. However, the wound area became much smaller in the 1/20 group on day 7, compared to the other two groups. After 14 days, the wound healing rate in the 1/20 group reached 86.29% ± 3.34%. In contrast, the wound healing rates were 69.20% ± 2.53% and 73.23% ± 3.18% in the blank and control group, respectively. Twenty-first days after surgery, the wound size in all groups was significantly reduced, especially in the 1/20 group, with more than 90% wound closure achieved (Fig. 6b).

To further assess the healing quality of the wounds and visualize the tissue regeneration, H&E staining was performed. As shown in Fig. 6c, the wound beds in all groups were filled by fibrin clots on day 3. Meanwhile, some fibroblasts and inflammatory cells started to infiltrate into the wound beds. On day 7, a large number of fibroblasts and inflammatory cells were observed in the newly formed granulation in all groups. Keratinocytes started to proliferate and migrate, forming a typical epidermal tongue at the wound edge. Fourteen days after surgery, few inflammatory cells were left in the wound bed in the 1/20 group, while there were still many in the blank and the control. On day 21, the wounds of the 1/20 group were covered entirely with the newly regenerated epidermis, whereas the re-epithelization in the blank and the control was severely delayed.

3.7.2. Keratinocyte proliferation in diabetic wounds

Proliferating keratinocytes were identified by examining the cell proliferation-associated nuclear antigen Ki67. As indicated by the red arrows in Fig. 7a, Ki67 positive cells were observed in the basal layer of the epidermal tongue in all groups on day 7, with more in the 1/20 group. On day 14, the number of Ki67 positive cells greatly increased in

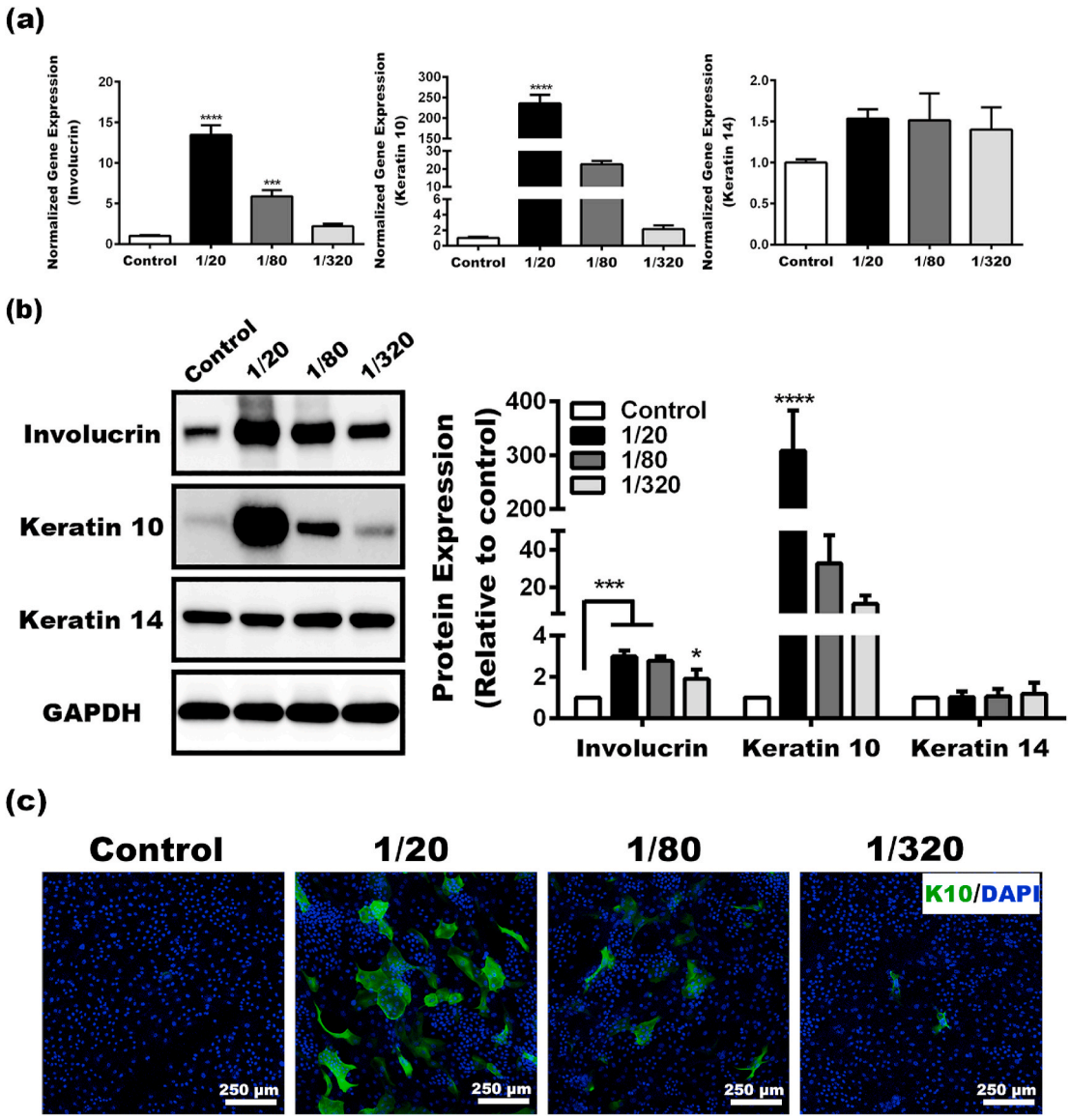

Fig. 4. The differentiation of keratinocytes in the BG extracts. qRT-PCR (a) and Western blot (b) analysis of key differentiation makers in keratinocytes. (c) Immunofluorescent staining of keratin 10 in keratinocytes. (*Statistically significant, *$p < 0.05$, ***$p < 0.001$, ****$p < 0.0001$ vs the control).

the blank and control groups. Consistently, the quantitative results also showed more Ki67 positive cells in the 1/20 on day 7 while fewer on day 14. Notably, proliferating keratinocytes in the blank and control group were found not only in the basal layer but also in the suprabasal layers. In contrast, fewer ki67 positive keratinocytes were seen in the 1/20 group, and all of them were limited in the basal layer.

3.7.3. Regeneration of epidermis in diabetic wounds

The differentiation of keratinocytes is the basis for forming the stratum corneum of the epidermis. Thus, the immunostaining for K14, K10, and involucrin was performed to determine the differentiation of keratinocytes in the newly formed epidermis. As shown in Fig. 7b, stronger expression of K10 and involucrin was detected in the 1/20 group than in the blank and control group, indicating a promoted keratinocyte differentiation by the BG extracts. Although the re-epithelialization failed to complete in the blank and control group, no difference was seen in keratin 14 expression in the epidermal layer of all groups. Next, the formation of TJs was evaluated through immunofluorescent staining of the key TJ proteins. The expression of ZO-1 and claudin-1 was significantly up-regulated in keratinocytes at the wound beds in the 1/20 group, compared to the blank and control groups (Fig. 7c). Almost all keratinocytes in the epidermal layer of the 1/20 group expressed both ZO-1 and claudin-1 at high levels. Particularly, claudin-1 in the 1/20 group was distributed along the plasma membrane between neighboring cells and organized into a continuous network structure, whereas claudin-1 in the blank and control group merely formed some “dotted lines”. According to our results, BG extracts promoted the differentiation of keratinocytes and enhanced the formation of TJs in the newly regenerated epidermis, which may help restore the barrier function of wounded skin.

4. Discussion

Re-epithelialization, which is achieved by the proliferation, migration, and differentiation of keratinocytes, is essential for successful wound closure [23]. However, this process is impaired in chronic wounds like diabetic foot ulcers due to the dysfunction of keratinocytes [24]. In this study, we found that the ionic extracts from 58S-BG promoted the collective migration, differentiation, and formation of TJs in cultured keratinocytes and diabetic rat wounds, thereby improving the

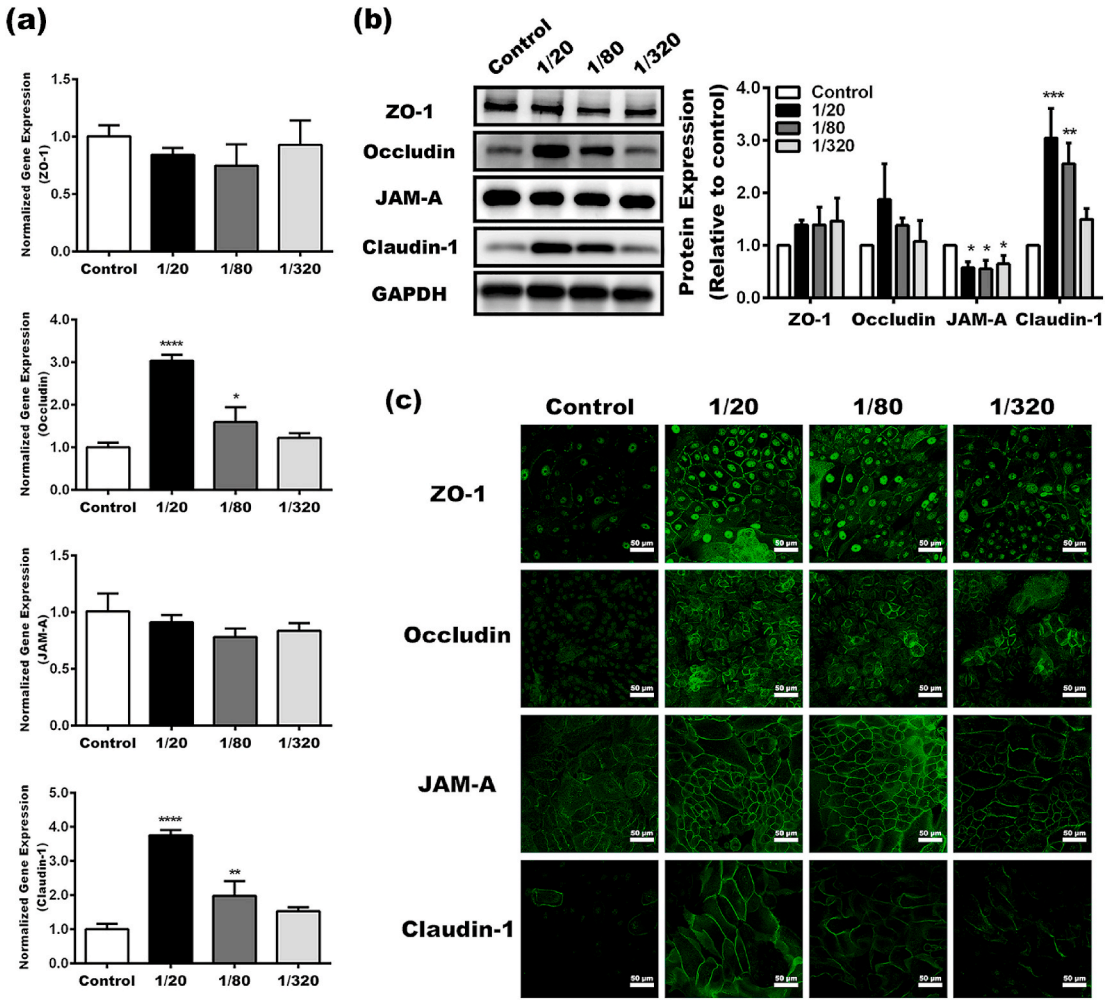

Fig. 5. The formation of tight junctions between keratinocyte in the BG extracts. qRT-PCR (a) and Western blot (b) analysis of key TJ proteins in keratinocytes. (c) The expression and localization of key TJ proteins in keratinocytes determined by immunofluorescence (*Statistically significant, *$p < 0.05$, **$p < 0.01$, ****$p < 0.001$,****$p < 0.0001$ vs the control).

re-epithelization and the restoration of the barrier function.

Upon skin injury, keratinocytes at the wound edge first loosen their adhesion to the basal lamina and start to crawl over the provisional wound matrix to close the defect in the epidermis. From the scratch assay in vitro, we found that, although keratinocytes in each group covered comparable wound areas in 24 h, they migrate in different ways. Specifically, BG extracts induced the collective migration of keratinocytes. Collective cell migration occurs when multiple cells move together as cohesive structures such as sheets, clusters, streams, or sprouts [25]. Unlike single cell migration during which cells dissociate and individually move around, cells during collective migration maintain their cell-cell contacts and move in a coordinated manner influenced by their neighboring cells. Because cells that migrate collectively are connected by cell-cell junctions like adherent and tight junctions, this type of migration may help recover the integrity and barrier function of the wounded skin. Actually, the epidermal tongue formed during the wound healing resulted from the collective migration of keratinocytes. Although cultured keratinocyte migrated at a similar rate in each group in the scratch assay, a faster re-epithelialization was observed in the diabetic rat wounds treated with 1/20 BG extracts, indicating BG extracts may affect the re-epithelialization through modulating not only keratinocytes but also other cells, such as fibroblast and macrophages. As the advancement of migrating epithelial tongue, keratinocytes start to proliferate to ensure an adequate supply of cells to close the wound. Only the basal keratinocytes can undergo division, while the terminally differentiated keratinocytes cannot. According to the CCK-8 assay results, BG extracts at low concentrations (1/80 and 1/320) exhibited little effects on the proliferation of cultured keratinocytes, while at high concentration (1/20), they inhibited cell proliferation. However, no obvious inhibition in keratinocyte proliferation was observed when 1/20 BG extracts were applied to diabetic rat wounds. This may be caused by the high metabolic activity and the large quantity of cells at the wound site. It is worth mentioning that one abnormality in keratinocytes in chronic wounds is that they usually exhibit a hyperproliferative phenotype [26]. In other words, mitotically active keratinocytes reside not only in the basal layer but also throughout the suprabasal layers. Consistently, proliferating keratinocytes, which are Ki67 positive, are found in both basal and suprabasal layers in the blank and control group on day 14 (Fig. 7a), indicating an abnormal phenotype of keratinocytes.

We next examined the barrier function of keratinocyte monolayers via the TEER measurement and the paracellular permeability assay. Surprisingly, BG extracts significantly enhanced the barrier function of the keratinocyte monolayers, as evidenced by the increased TEER value and the decreased paracellular permeability (Fig. 3). To explore the underlying mechanism involved in the enhanced barrier function by the BG extracts, both the differentiation and formation of TJs in keratinocytes were evaluated. The elevated expression of both K10 and involucrin demonstrated that the BG extracts promoted the differentiation of keratinocytes in vitro and in vivo (Figs. 4 and 7b). It was noted that

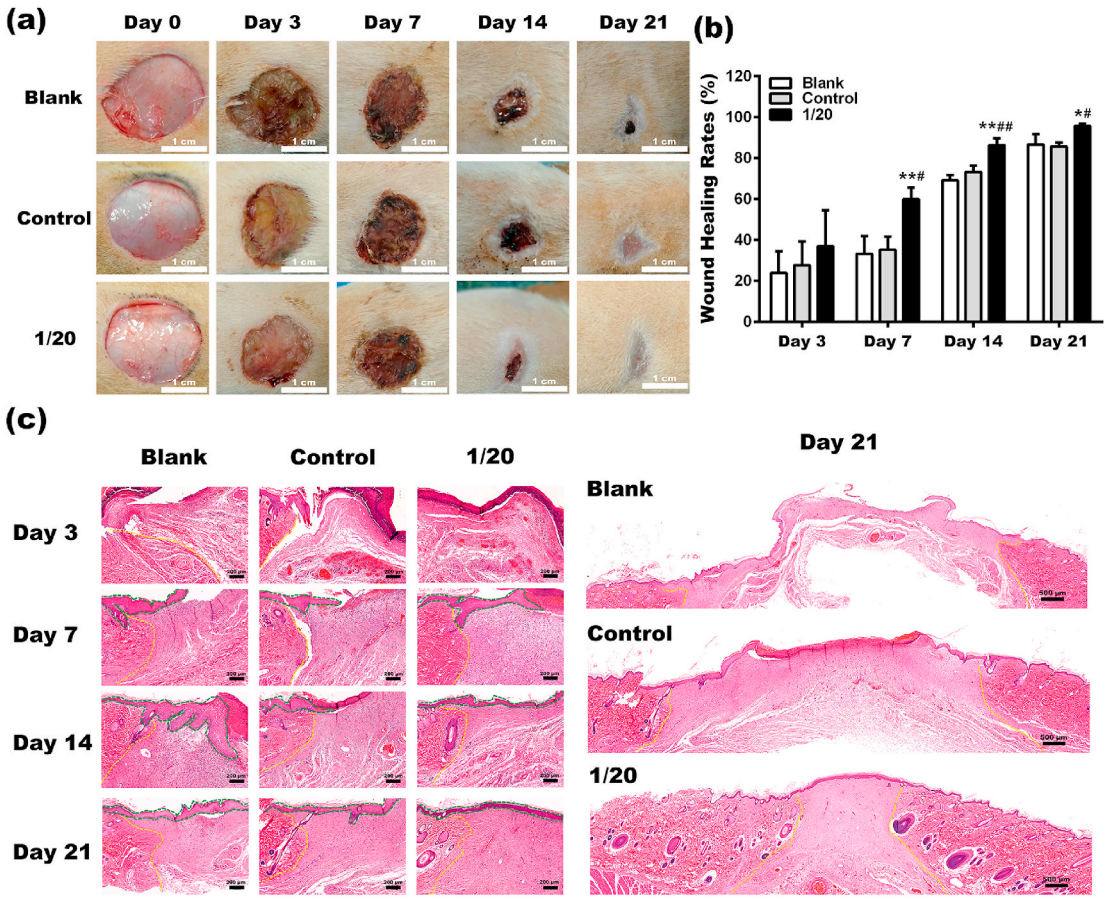

Fig. 6. (a) Representative images of the Blank, Control and 1/20 groups during wound healing. (b) Wound healing rate at each time point. (c) HE staining images of wound tissues in each group on day3, day7, day14 and day21 after surgery. The yellow dotted line is the boundary between normal tissue and healing tissue, and the newly formed epidermis is outlined with a green dotted line (*Statistically significant, *$p < 0.05$, **$p < 0.01$ vs the blank group, #Statistically significant, #$p < 0.05$, # #$p < 0.01$ vs the control group).

keratin 10 positive keratinocytes were highly concentrated in some area rather than evenly distributed (Fig. 4c). The reason for this phenomenon is that not all keratinocytes in the culture differentiate at the same rate. Under the stimulation of BG extracts, keratinocytes tend to cluster at higher densities in some area. It has been reported that high cell densities promote the differentiation of cultured keratinocytes by endogenous activation of the protein kinase C signaling pathway [27]. Consistently, keratin 10 positive keratinocytes were highly concentrated in area with higher cell densities. Since the degree of differentiation is an important factor that affects cell mitotic activity, the inhibited proliferation rate of keratinocytes in BG extracts may partially result from the enhanced differentiation. As for the formation of TJs, the expression and localization of four major TJ proteins, including claudin-1, occludin, JAM-A, and ZO-1, were determined. The expression of claudin-1 was elevated in the 1/20 and 1/80 groups compared to the control. Interestingly, it was noted that the BG extracts did not change the mRNA level of JAM-A in keratinocytes while decreased its protein level, indicating a post-transcriptional regulation mechanism of the BG extracts on the expression of JAM-A. More important, the BG extracts stimulate all these four TJ proteins to assemble into TJs located along the edge of the cell membrane (Fig. 5c). Thus, both the differentiation and formation of TJs in keratinocytes were involved in mediating the enhanced barrier function of the keratinocyte monolayers. Although the barrier function of the newly generated epidermis at the diabetic wounds was not measured due to the lack of necessary equipment, the elevated expression of both the differentiation markers and the TJ markers indicated BG extracts enhanced the integrity and barrier function of the epidermis. In addition to their well-recognized roles in maintaining barrier functions, TJs affect the wound healing process through regulating cell proliferation, migration, and differentiation, as well as immune response and homeostasis. For instance, claudin-1 knockdown leads to delayed migration and reduced proliferation of keratinocytes through attenuating the activation of AKT signaling pathway [8]. Loss of occludin results in disorganization of the actin cytoskeleton and reduced cell protrusion, which is required for cell migration [28]. The inhibition of JAM-A reduces fibroblast growth factor (FGF-2)-induced proliferation and migration of endothelial cells, thus suppressing angiogenesis [29]. The enhanced formation of TJs between keratinocytes in the BG extracts also provides a possible explanation for the observed collective cell migration. Claudin-1 has been reported to increase cell cohesion, and consequently facilitate the collective migration of cancer cells, which correlate with invading and metastasis of tumors [30,31]. Occludin was also showed to promote cell collective migration [28].

What are the potential underlying mechanisms for the regulation of BG extracts on the barrier functional behaviors of keratinocytes? Substantial researches have shown that calcium ions are a crucial modulator of both keratinocyte differentiation and TJs [32–34]. Calcium may induce keratinocyte differentiation via both genomic and non-genomic pathways. An example of a genomic mechanism involves the activation of the calcium-responsive promoters such as activator protein 1 (AP1) sites found in the involucrin and in the keratin 1 gene [33]. With respect to TJs, calcium may alter the integrity of TJs by a number of different signal transduction cascades (*eg.* PKC signaling), as well as via direct interaction of calcium ions with junction proteins [34]. Considering that the concentration of Calcium ions in the BG extracts was much higher than that in control (Table 1). Thus, calcium ions released from

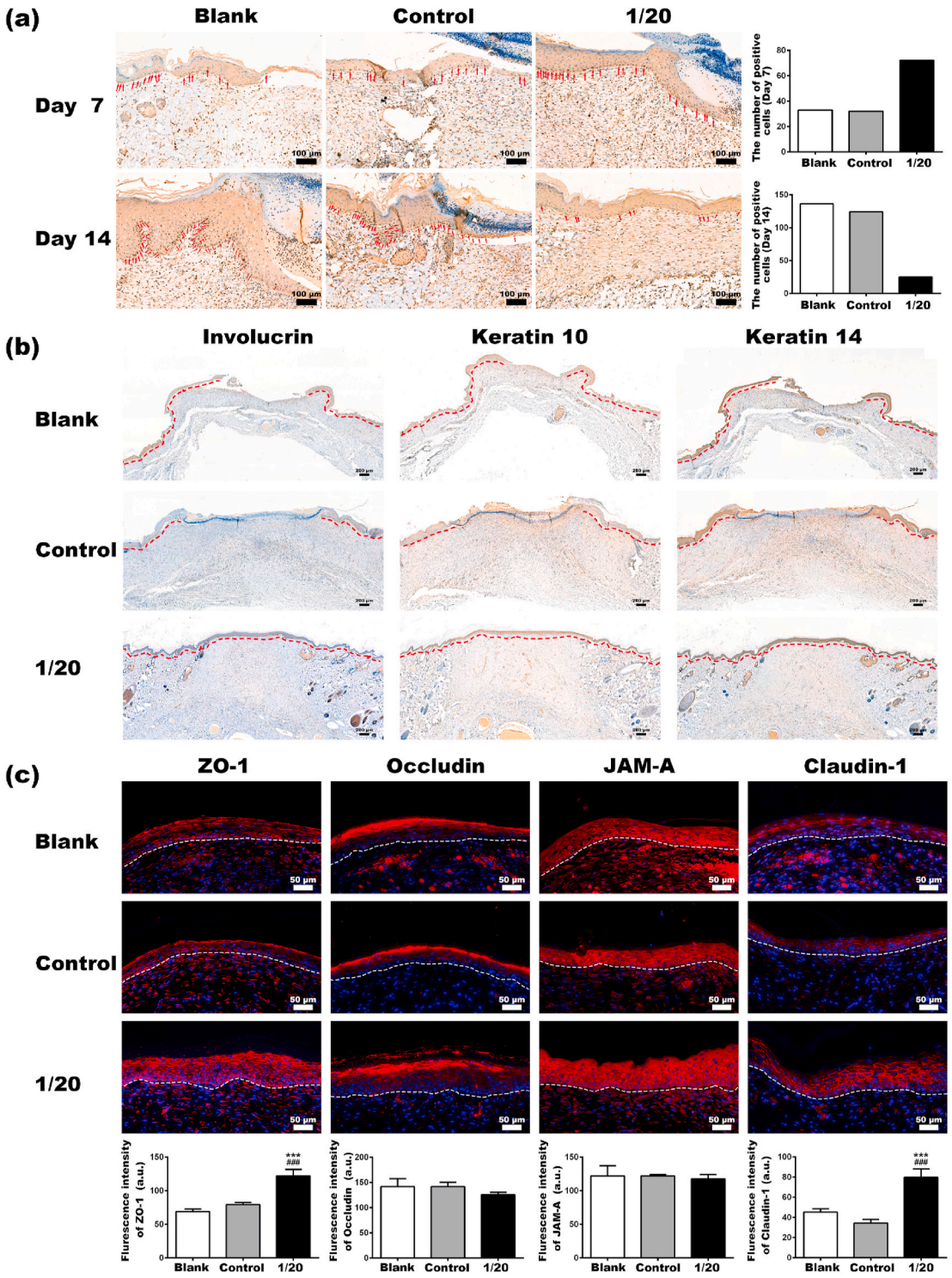

Fig. 7. (a) Immunohistochemical staining and quantitative analysis of Ki67 of wound sections. The red arrows indicate the Ki67 positive cells. (b) Immunohistochemical staining of Involucrin, Keratin 10 and Keratin 14 of wound sections on day 21. The newly formed epidermis is outlined with a red dotted line. (c) Immunofluorescent staining and quantitative analysis of ZO-1, Occludin, JAM-A and Claudin-1 of wound sections on day 21 (*Statistically significant, *$p < 0.05$, ***$p < 0.001$ vs the blank group, $^{\#}$Statistically significant, $^{\#}p < 0.05$, $^{\#\#\#}p < 0.001$ vs the control group).

the BG particles may be involved in mediating the promoted cell differentiation and TJ formation by BG extracts. But further studies are needed to reveal the regulatory role of other ions in the BG extracts, such as Silicon ions.

5. Conclusion

In this study, we explored the regulatory role of BG extracts on the barrier related functions of keratinocytes. Our results demonstrated that BG extracts induced the collective migration of keratinocytes, increased the TEER of keratinocyte monolayers, and reduced the paracellular permeability, all of which indicated an enhanced barrier function of the

keratinocyte monolayers. Further investigation illustrated this positive functional change may resulted from the promoted keratinocyte differentiation and the assembly of tight junctions between keratinocytes by BG extracts. Moreover, our in vivo study showed that BG extracts accelerated re-epithelization, stimulated the keratinocyte differentiation, and increased tight junctions in the newly regenerated epidermis in diabetic rat wounds.

CRediT authorship contribution statement

Fengling Tang: Investigation, Formal analysis, Writing – original draft. **Junliang Li:** Validation, Formal analysis. **Weihan Xie:** Investigation. **Yunfei Mo:** Investigation. **Lu Ouyang:** Investigation. **Fujian Zhao:** Validation. **Xiaoling Fu:** Conceptualization, Project administration, Writing – review & editing, Funding acquisition. **Xiaofeng Chen:** Supervision, Funding acquisition.

Declaration of competing interest

There are no conflicts to declare.

Acknowledgements

This work was financially supported by the National Key R&D Program of China (2017YFC1105000), the National Natural Science Foundation of China (51672088, 31971266, U1801252), the Key Research and Development Program of Guangzhou (202007020002), the Natural Science Foundation of Guangdong Province (2019A1515110480), the Science and Technology Program of Guangzhou (201804020060), and Fundamental Research Funds for the Central Universities.

Appendix A. Supplementary data

Supplementary data to this article can be found online at https://doi.org/10.1016/j.bioactmat.2021.02.041.

References

[1] M. Cork, J. Dermatol. Treat. 8 (1997) S7–S13.
[2] C. Zihni, et al., Nat. Rev. Mol. Cell Biol. 17 (9) (2016) 564–580.
[3] H. Chiba, et al., Biochim. Biophys. Acta 1778 (3) (2008) 588–600.
[4] L. Gonzalez-Mariscal, et al., Prog. Biophys. Mol. Biol. 81 (1) (2003) 1–44.
[5] M.L. Usui, et al., J. Histochem. Cytochem. 56 (7) (2008) 687–696.
[6] K.A. Kim, et al., Laryngoscope 128 (12) (2018) E393–E401.
[7] Q.W. Jiang, et al., Acta Pharmacol. Sin. 40 (9) (2019) 1205–1211.
[8] T. Volksdorf, et al., Am. J. Pathol. 187 (6) (2017) 1301–1312.
[9] H. Yu, et al., ACS Appl. Mater. Interfaces 8 (1) (2016) 703–715.
[10] W. Xie, et al., J. Mater. Chem. B 7 (6) (2019) 940–952.
[11] X. Dong, et al., J. Mater. Chem. B 5 (26) (2017) 5240–5250.
[12] C. Mao, et al., Biomed. Mater. 10 (2) (2015).
[13] H. Li, et al., Biomaterials 84 (2016) 64–75.
[14] A. Hoppe, et al., Biomaterials 32 (11) (2011) 2757–2774.
[15] J. Chen, et al., Bioactive materials 3 (3) (2018) 315–321.
[16] L. Zhang, et al., Exp. Cell Res. 341 (2) (2016) 157–165.
[17] B. Srinivasan, et al., Jala 20 (2) (2015) 107–126.
[18] A. Leguina-Ruzzi, et al., Dermatoendocrinol 9 (1) (2017), e1267078.
[19] M. Cao, et al., PloS One 8 (5) (2013), e61944.
[20] L. Sun, et al., J. Mater. Chem. B 9 (5) (2021) 1395–1405.
[21] D.D. Bikle, J. Cell. Biochem. 92 (3) (2004) 436–444.
[22] R.L. Eckert, et al., J. Invest. Dermatol. 123 (1) (2004) 13–22.
[23] L. Koivisto, et al., Endod. Top. 24 (2011) 59–93.
[24] S.C.S. Hu, et al., J. Dermatol. Sci. 84 (2) (2016) 121–127.
[25] P. Rorth, EMBO Rep. 13 (11) (2012) 984–991.
[26] I. Pastar, et al., Adv. Wound Care 3 (7) (2014) 445–464.
[27] Yun-Sil, et al., J. Invest. Dermatol. 111 (5) (1998) 762–766.
[28] D. Du, et al., Dev. Cell 18 (1) (2010) 52–63.
[29] V.G. Cooke, et al., Arterioscler. Thromb. Vasc. Biol. 26 (9) (2006) 2005–2011.
[30] P. Dhawan, et al., J. Clin. Invest. 115 (7) (2005) 1765–1776.
[31] B.W. Zhou, et al., J. Clin. Med. 4 (12) (2015) 1960–1976.
[32] D.D. Bikle, et al., Expet Rev. Endocrinol. Metabol. 7 (4) (2012) 461–472.
[33] E. Floriana, et al., Eur. J. Dermatol. 24 (6) (2014) 650–661.
[34] R.C. Brown, et al., Stroke 33 (6) (2002) 1706–1711.